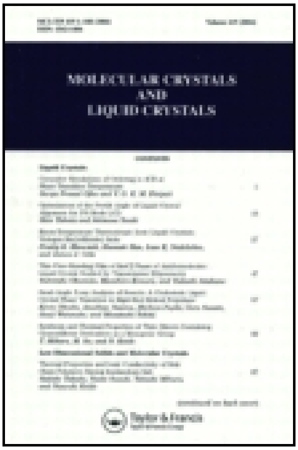

Molecular Crystals and Liquid Crystals
Publication details, including instructions for authors and subscription information:
http://www.tandfonline.com/loi/gmcl20

Microcup Array Fabricated by Thermal Imprint Lithography for E-Paper Application

Jeongbok Kwak [a], Sangmoon Lee [a], Yongsoo Oh [a] & Hwan-Soo Lee [a]
[a] Central R&D, Samsung Electro-Mechanics, Youngtong-gu, Suwon, Kyunggi-do, Korea

Version of record first published: 10 Nov 2009

To cite this article: Jeongbok Kwak, Sangmoon Lee, Yongsoo Oh & Hwan-Soo Lee (2009): Microcup Array Fabricated by Thermal Imprint Lithography for E-Paper Application, Molecular Crystals and Liquid Crystals, 514:1, 219/[549]-227/[557]

To link to this article: http://dx.doi.org/10.1080/15421400903240878

Mol. Cryst. Liq. Cryst., Vol. 514, pp. 219/[549]–227/[557], 2009

ISSN: 1542-1406 print/1563-5287 online
DOI: 10.1080/15421400903240878

Microcup Array Fabricated by Thermal Imprint Lithography for E-Paper Application

Jeongbok Kwak, Sangmoon Lee, Yongsoo Oh, and Hwan-Soo Lee
Central R&D, Samsung Electro-Mechanics, Youngtong-gu, Suwon, Kyunggi-do, Korea

Thermal imprinting method was developed to provide a microcup array for the application to e-paper, and the imprinted feature was investigated as functions of time and temperature. Even in a short period of time of 2 second, the pattern was imprinted onto a resin to the full depth at a temperature higher than $T/T_g = 0.64$ (where the T_g is 156°C), however, the hardening process as long as 30 minutes appears to be necessary to achieve the full mechanical strength. We propose a roller imprint process that suffices the two experimental observations and is put to practical use. A large array of microcup having typical dimension in the range of 60–100 μm in width or length, 20–40 μm in height, and 10–20 μm in width of partition walls was able to be fabricated via the roller imprint method.

Keywords: e-paper; microcup; roller imprint; thermal imprint

INTRODUCTION

Recently, electronic paper display (EPD) which enables thin, flexible, low-power, and electronically updateable imaging has been of great interest. One type of EPD is associated with the use of electrophoresis for creating an image.

A Microcup® type electrophoretic film is one example of electrophoretic display [1]. The microcup array, which is typically a square grid of rib structure, is formed to limit the lateral particle migration for this application, and then an electrophoretic fluid containing pigment particles and dye was filled in the microcup with an overcoat on top for sealing. One approach for creating the rib structure recently

Address correspondence to Dr. Hwan-Soo Lee, Central R&D Institute, Samsung Electro-Mechanics, 314 Maetan-dong, Youngtong-gu, Suwon, Kyunggi-do, South Korea. E-mail: hwansoo725.lee@samsung.com

proposed is to utilize microreplication through imprint (or embossing). An interesting feature of their process is that microreplication is carried out via roll-to-roll (R2 R) process. Imprint technique, in particular, as R2 R process is combined, provides an extremely simple and cost-effective means [2–4].

In thermal imprint lithography, a thermoplastic polymer (or resin) is heated above its glass transition temperature (T_g) before the pressure is exerted onto the stamp. After the temperature has reached to a preprogrammed value, a pressure is applied and the temperature is maintained constant to let the polymer flow and adapt patterns of the stamp. As the pattern is transferred in a complete fashion, the resin cools down below the T_g, and the stamp is lifted from the resin.

In Figure 1, imprinted patterns are shown. The inset indicates typical temperature and pressure profiles during an imprint cycle where a pressure of 1 MPa is applied for 40 minutes. As illustrated above, it takes quite a time to perform the entire steps of thermal imprint. Time becomes even longer as cooling slows down to sufficiently relax stress created during imprint. Stress induced at a stage of imprint often generates defects in pattern or, even seriously, can result in fracture in pattern [5].

In this study, a microcup array was fabricated through thermal embossing process. We present details of experimental results performed by controlling two important parameters, temperature and time during imprint. Through this study, we aim to propose an

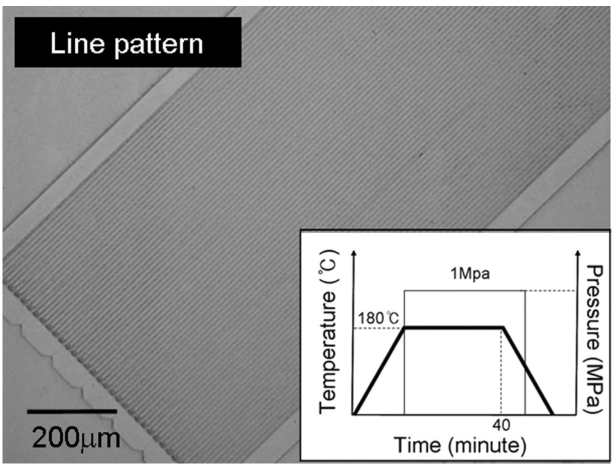

FIGURE 1 Imprinted line patterns by a typical imprint process. The inset indicates typical profiles of temperature and pressure.

optimal R2 R process which is suitable for high throughput as thermal imprint lithography is employed in the fabrication of microcup array.

EXPERIMENTAL

For fabricating a large array of microcup, a commercially available Novolac type epoxy-based resin (GX-13, Ajinomoto) was laminated on either flexible or rigid substrates. The resin contained an inorganic filler (SiO_2), a difunctional monomer to allow crosslinking, and a low molecular weight monomer to reduce viscosity. The filler provided additional mechanical strength, and the filler content in the resin was about 38 vol.%. The T_g of the resin was 156°C. Either Ni or polymer stamps were used to imprint patterns onto the resin.

Figure 2 shows temperature and pressure profiles employed in the fabrication of micro-pattern in this study. The cycle consists of Steps A (embossing) and B (hardening or curing). Prior to embossing, the resin was heated to provide a viscoelastic behavior [6–7]. During Step A, the viscosity was low enough to let the polymer flow and ensure the pattern imprinted to the full depth. In Step B, the resin was heated up to, typically, 180°C for 30 minutes. This step was needed to achieve higher mechanical strength and stability of imprinted structures through crosslinking of the resin. A pressure of 1 MPa was continuously applied during both imprinting and hardening. It should be noted that a pattern would collapse if hardening is performed with the stamp lifted up.

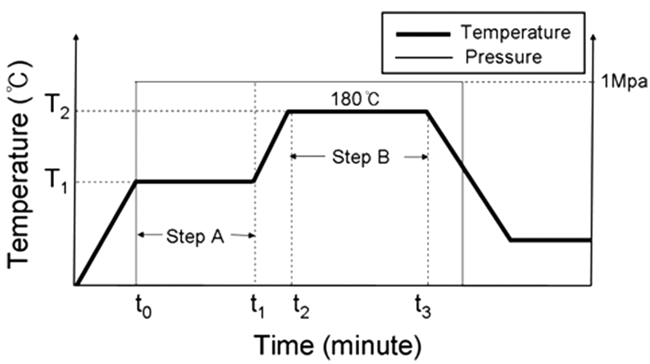

FIGURE 2 Profiles of temperature and pressure with respect to imprinting time. Steps A and B correspond to imprinting (embossing) and hardening (curing), respectively.

In some cases, line patterns were examined to simplify the interpretation. It is expected that the observations for the line pattern may apply to a square grid of microcup structure as well.

MEASUREMENTS

A rheometer (AREA, TA instrument) was used to measure the rheological behavior of the epoxy resin. Thermal properties of the resin were studied by using a thermal mechanical analyzer (TMA Q400, TA instrument), which allowed us to estimate the T_g. A 3-dimensional profile microscope (VK-9510, Keyence) using a violet laser was used to measure a pattern profile after microreplication. Scanning electron microscopy (SEM) was also used to quantify the dimension of imprinted features. Tensile strength was measured, using a universal tensile machine (Model 4206, Instron). For the sample preparation, curing was carried out at a temperature of 180°C. Prior to the curing, two sheets of the resin were overlaid each other, and pressurized with a pressure of 1 MPa for ten minutes with no embossing performed. After the hardening, 'dog bone' specimens with a length of 12 cm were prepared for the test of tensile strength.

RESULTS AND DISCUSSION

In Figure 3, a pattern height as a function of temperature (T_1) at Step A is shown. A pressure of 1 MPa was applied for two seconds.

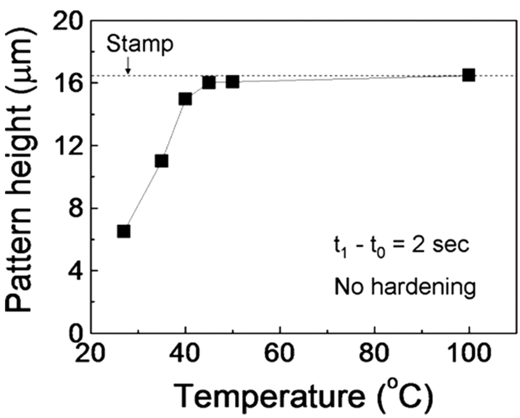

FIGURE 3 Pattern height vs. temperature during imprint. An increase in pattern height was observed as the temperature increased. The applied pressure and the imprinting time during Step A were fixed to 1 MPa and 2 seconds.

The shortest time to control during imprint was about two seconds. No curing process that corresponds to Step B was carried out for this investigation. With increasing temperature, the pattern height begun to increase, and was leveled off at a higher temperature. Even a short period of time of two seconds at a temperature greater than 50°C was sufficient to transfer the pattern near completion. At a temperature (T_1) of 100°C that corresponds to $T_1/T_g = 0.64$, the pattern was imprinted to the full depth. The dotted line in Figure 3 indicates the corresponding pattern depth on the stamp. The result implies that the pattern transfer is possible within a quick process time (<2 seconds) and at a temperature below the T_g. Nonetheless, it is somewhat surprising that the pattern is formed even at room temperature (RT). The lower bound of the pressure the equipment can apply on the stamp was 1 MPa.

In Figure 4, the pattern height is shown as functions of temperature and time. At a temperature as high as 100°C, which corresponds to a viscosity of ~3500 Pa·sec, the cavity on the stamp was rapidly filled with the polymer to the full depth. At a lower temperature, the imprinting time dependence of the pattern height is apparent since a sufficiently low viscosity is not likely to be obtained in this range. Other important factors determining pattern height can arise from applied pressure, imprinted area, and resin thickness.

In Table 1, a ratio (R) of a pattern height to the corresponding stamp height is shown as functions of imprinting time ($t_1 - t_0$) and temperature (T_1) at step A where a pressure of 1 MPa was applied.

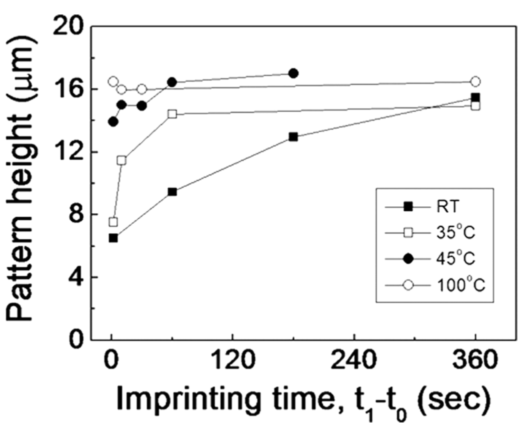

FIGURE 4 Pattern height vs. imprinting time for different temperatures during imprint.

TABLE 1 Ratio (R) of Pattern Height to Stamp Height as Functions of Imprinting Time ($t_1 - t_0$) and Temperature (T_1) at Step A. A Pressure of 1 MPa was Applied. No Step B was Carried Out

T_1 (°C)	$t_1 - t_0$ (sec)	R (1 MPa)
RT	2	0.42
35	2	0.50
45	2	0.82
100	2	1.00

No curing process (step B) was carried out. The ratio increased from 0.42 to 1.00 in going from RT to 100°C.

In Table 2, a ratio (R) of a pattern height to the stamp height is shown as functions of imprinting time ($t_3 - t_2$) and temperature (T_2) at step B. Step A in Table 1 was carried out prior to step B. Two cases (no pressure and 1 MPa) at step B were compared. The ratio of 1 was observed for both of the cases, indicating the patterns were formed to the full depth. Note that the ratio of 1 was obtained even without pressure at step B. This strongly suggests that another factor other than compression play a role in completing the pattern. We attribute this to capillary force at work during Step B. Details with regard to role of capillary force in imprinting microcup arrays will be a future subject of publication.

In Figure 5, mechanical strength of the resin was examined with varying a time ($t_3 - t_2$) for hardening. The tensile strength of ~80 MPa was observed as the resin was fully cured. It took more than 30 minutes of curing. When a specimen was subjected to tensile load, the specimen underwent initial elongation, and a further increase that

TABLE 2 Ratio (R) of Pattern Height to Stamp Height as Functions of Imprinting Time ($t_3 - t_2$) and Temperature (T_2) at Step B. Step A in Table 1 was Carried Out Prior to Step B. Two Cases (No Pressure and 1 MPa) at Step B were Compared

T_1 (°C)	$t_1 - t_0$ (sec)	T_2 (°C)	$t_3 - t_2$ (min)	R (no pressure)	R (1 MPa)
RT	2	180	30	1.00	1.00
35	2	180	30	1.00	1.00
45	2	180	30	1.00	1.00
100	2	180	30	1.00	1.00

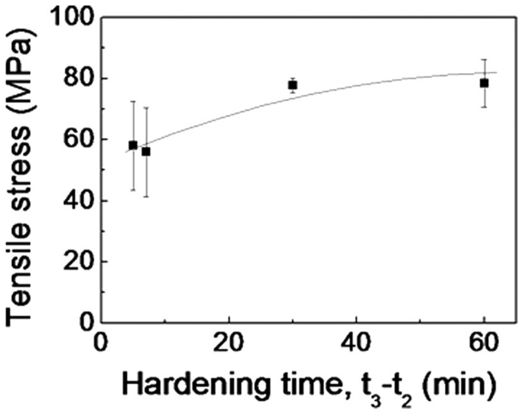

FIGURE 5 Tensile stress as a function of hardening time. More than 30 minutes were taken for the resin to be fully hardened.

exceeded a certain value eventually ruptured the specimen. The critical strain at break was around ~2.5% or less.

In Figure 6, two roller imprinting processes (RIPs) where the two observations (embossing can be quick, however, hardening should be rather long) are carefully reflected is schematically drawn. As shown

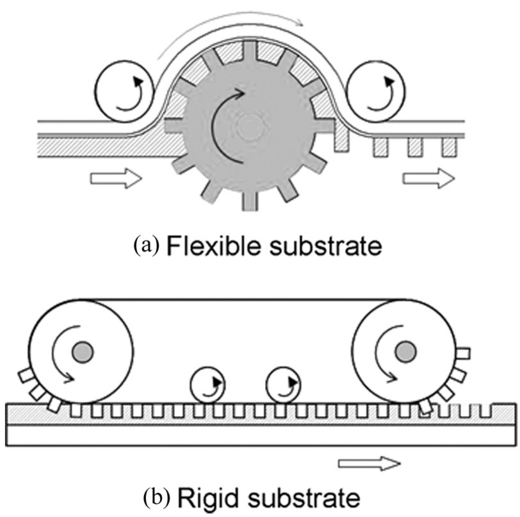

FIGURE 6 Two proposed roller imprint processes. One is applicable to flexible substrates and the other for rigid substrates.

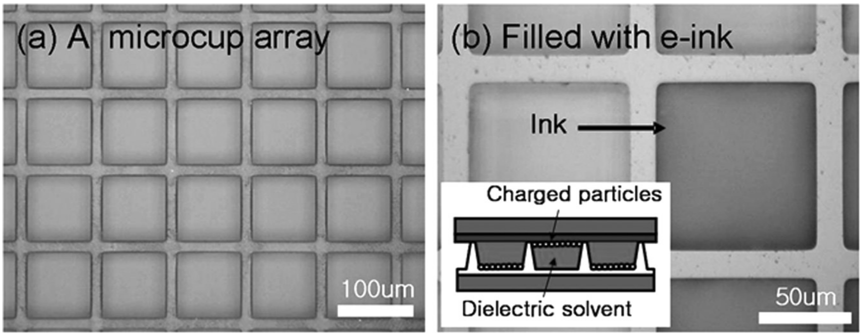

FIGURE 7 (a) Imprinted microcup array before ink injection and (b) after ink injection. Microcup types of patterns were successfully transferred onto a thermo-set resin with high fidelity.

in Figure 6(a), for a flexible substrate, the first contact roller brings the substrate into contact with the patterned roll stamper, and the other roller keeps the contact while becoming hardened. For a rigid substrate [see Figure 6(b)], a stamper in a sheet form which is flat but bendable is used. In particular, this design permits high throughput since a faster roller speed as well as a longer contact between the stamper and the substrate are simultaneously allowed.

Figure 7(a) shows that formation of microcup patterns was successfully demonstrated onto the resin, using a RIP. The microcup array typically had dimension in the range of 60–100 μm in width or length, 20–40 μm in height, and 10–20 μm in width of partition walls. It should be emphasized that the pattern possessed an aspect ratio of 2 to 1 or less. The ratio greater than 2 often caused a poor demolding characteristic.

In Figure 7(b), microcups are magnified. Some areas are filled with e-ink, which is displayed in blue. In fabricating EPD, filling and sealing e-ink into an individual microcup are another critical steps, and generally very time-consuming. An inkjet process can be employed for this purpose, however, we confine the issue discussed here to the microcup fabrication by imprinting.

CONCLUSION

The viscosity of the resin at a given temperature and an imprinting time largely determined the pattern height. At a higher viscosity (that is, a lower temperature of T_1 at Step A), the longer imprinting time was required to imprint the pattern to the full depth. Two roller imprint methods that are applicable to either flexible or rigid substrates were proposed, based upon the two observations made (embossing can be quick within a few seconds, however, hardening should be at least as long as 30 minutes). Employing a roll-type imprint can be promising in the fabrication of a microcup array, and be an alternative to conventional imprint technique for a large-scale micro-patterning.

REFERENCES

[1] Zang, H. M. & Liang, R. C. (2003). *Spectrum*, *16*(2), 16.
[2] Liang, R. C., Hou, J., Chung, J., Wang, X., Pereira, C., & Chen, Y. (2003). *SID 03' Digest*, paper *20*(1), 838.
[3] Chou, S. Y., Krauss, P. R., & Renstrom, P. J. (1995). *Appl. Phys. Lett.*, *67*, 3114.
[4] Inoue, S., Kawai, H., Kanbe, S., Saeki, T., & Shimoda, T. (2002). *IEEE Trans. Electron Devices*, *4*(8), 1532.
[5] Hirai, Y., Yoshida, S., & Takagi, N. (2003). *J. Vac. Sci. Technol. B*, *21*(6), 2765.
[6] Scheer, H.-C., Bogdanski, N., Wissen, M., & Mollenbeck, S. (2007). *J. Vac. Sci. Technol. B*, *25*, 2392.
[7] Gottschalch, F., Hoffmann, T., Torres, C. S., Schulz, H., & Scheer, H.-C. (1999). *Soild-State Electron.*, *43*, 1079.